

Three-body break-up in deuteron-deuteron scattering at 65 MeV/nucleon

A. Ramazani-Moghaddam-Arani^{1,2,a}, H.R. Amir-Ahmadi¹, A.D. Bacher³, C.D. Bailey³, A. Biegun¹, M. Eslami-Kalantari^{1,4}, I. Gašparić⁵, L. Joulaeizadeh¹, N. Kalantar-Nayestanaki¹, St. Kistryn⁶, A. Kozela⁷, H. Mardanpour¹, J.G. Messchendorp¹, A.M. Micherdzinska⁸, H. Moeini¹, S.V. Shende¹, E. Stephan⁹, E.J. Stephenson³, and R. Sworst⁶

¹ KVI, University of Groningen, Groningen, The Netherlands

² Department of Physics, Faculty of Science, University of Kashan, Kashan, Iran

³ Indiana University Cyclotron Facility, Bloomington, Indiana, USA

⁴ Department of Physics, Faculty of Science, Yazd University, Yazd, Iran

⁵ Rudjer Bošković Institute, Zagreb, Croatia

⁶ Institute of Physics, Jagiellonian University, Cracow, Poland

⁷ Henryk Niewodniczański Institute of Nuclear Physics, Cracow, Poland

⁸ University of Winnipeg, Winnipeg, Canada

⁹ Institute of Physics, University of Silesia, Katowice, Poland

Abstract. We successfully identified a few final states in deuteron-deuteron scattering at 65 MeV/nucleon at KVI using a unique and advanced detection system called BINA. This facility enabled us to perform cross sections and polarization measurements with an excellent statistical and systematical precision. The analysis procedure and part of the results of the three-body break-up channel in deuteron-deuteron scattering at 65 MeV/nucleon are presented in this paper.

The physics phenomena of nuclei are for a large part understood by considering the interaction between its building elements, the nucleons. In 1935 Yukawa described the nucleon-nucleon (NN) force with an exchange of massive mesons [1] similar to the electromagnetic interaction which can be represented by an exchange of a massless photon. Few phenomenological nucleon-nucleon potentials have been derived based on Yukawa's theory and are able to reproduce more than 4000 data points in neutron-proton and proton-proton scattering with extremely high precision. These so-called high-quality NN potentials are used in Faddeev [2,3] equations to have exact solution for a three-nucleon system. Already for the simplest three-nucleon system, the triton, an exact solution of the three-nucleon Faddeev equations employing two-nucleon forces (2NFs) underestimates the experimental binding energy [4], showing that 2NFs are not sufficient to describe the three-nucleon system accurately by the presence of a third nucleon. The existence of an additional force, the three-nucleon (3N) interaction, was predicted by Primakov [5] and was proven rigorously by a comparison between precision data and state-of-the-art calculations. In general, adding 3NF effects to the NN potentials gives a better agreement between cross section data in proton-deuteron scattering and corresponding calculations [6,7,8,9,10,11,12,13,14,15,16,17], whereas a comparison for the corresponding spin observables yields various discrepancies [7,8,9,18,19,20,21,22]. This demon-

strated that spin-dependent parts of the 3NFs are poorly understood and that more studies in this field are needed.

The 3NF effects are in general small in the three-nucleon system. A complementary approach is to look into systems for which the 3NF effects are significantly enhanced in magnitude. For this, it was proposed to study the four-nucleon system. The experimental database in the four-nucleon system is presently poor in comparison with the three-nucleon system. Most of the available data were taken at very low energies, in particular below the three-body break-up threshold of 2.2 MeV. Also, theoretical developments are evolving rapidly at low energies [23,24,25,26], but lag behind at higher energies. The experimental database at intermediate energies is very limited [27,28,29]. This situation calls for extensive four-nucleon studies at intermediate energies. The goal of our work was to perform a comprehensive measurement of cross sections and spin observables in various $d+d$ scattering processes at 65 MeV/nucleon, namely the elastic and three-body break-up channels. With these data, we have drastically enriched the four-nucleon scattering database. The extensive database of spin and cross section observables in various deuteron-deuteron scattering processes together with precise and ab-initio calculations can potentially reveal many details of 3NF effects.

Deuteron-deuteron scattering below the pion-production threshold leads to 5 possible final states with a pure hadronic signature, namely

^a e-mail: ramazani@kvi.nl

1. Elastic channel: $\mathbf{d} + d \rightarrow d + d$;

2. Neutron-transfer channel: $\mathbf{d} + d \rightarrow p + t$;
3. Proton-transfer channel: $\mathbf{d} + d \rightarrow n + {}^3\text{He}$;
4. Three-body final-state break-up: $\mathbf{d} + d \rightarrow p + n + d$;
5. Four-body final-state break-up: $\mathbf{d} + d \rightarrow p + n + p + n$.

In this work, the three-body final-state break-up in deuteron-deuteron scattering is further referred as the three-body break-up. The study and identification of these final states requires an experimental setup with specific characteristic, namely, a large phase space coverage, a good energy and angular resolution, and the ability of particle identification (PID). The experiment presented in this paper was carried out using the Big Instrument for Nuclear-polarization Analysis, BINA, which has these requirements [30]. A polarized beam of deuterons with a kinetic energy of 65 MeV/nucleon was impinging on a liquid deuterium target. The elastic, neutron-transfer and three- and four-body break-up channels were identified using the energy, scattering angles and time-of-flight (TOF) information. We, only, discuss the three-body break-up channel in this paper.

For the analysis of the three-body break-up data we measured the energies, polar and azimuthal angles of the two coincident, emitted particles. Using the measured variables and considering momentum and energy conservation, all the other kinematical variables of the reaction can be obtained unambiguously. The kinematics of the three-body break-up reaction are determined by using the scattering angles of the proton and the deuteron ($\theta_d, \theta_p, \phi_{12} = |\phi_d - \phi_p|$) and the correlation between their energies presented by the kinematical curve which is called the S -curve. The energies of the proton, E_p , and deuteron, E_d , were described as a function of two new variables, D and S . The variable S is the arc-length along the S -curve with the starting point chosen arbitrarily at the point where E_d is minimum and D is the distance of the (E_p, E_d) point from the kinematical curve. The S -curves for several kinematical

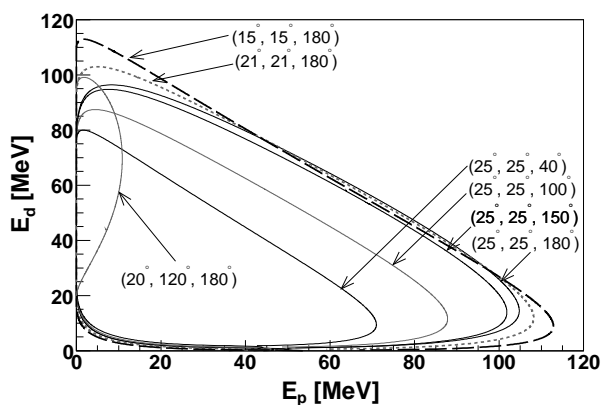


Fig. 1. The energy correlation between protons and deuterons in coincidence for the three-body break-up reaction in $\mathbf{d} + d$ scattering is shown as S -curves for several kinematical configurations. The kinematics are defined by $(\theta_d, \theta_p, \phi_{12})$, the polar scattering angles of the proton and deuteron, respectively, and the relative azimuthal angle.

cal configurations are shown in Fig. 1. Each S -curve is labeled by three numbers. For example, the label $(20^\circ, 30^\circ, 180^\circ)$ shows a coincidence between a deuteron that scatters to 20° and a proton that scatters to 30° , and the azimuthal opening angle, ϕ_{12} , between the deuteron and the proton is 180° .

The first step in the event selection for the three-body break-up channel is to find the energy correlation between the final-state protons and deuterons for a particular kinematical configuration $(\theta_p, \theta_d, \phi_{12})$, where θ_p and θ_d are the polar angles of the proton and the deuteron, respectively, and ϕ_{12} is the difference between their azimuthal angles. The number of break-up events in an interval $S - \frac{\Delta S}{2}$ and $S + \frac{\Delta S}{2}$ was obtained by projecting the events on a line perpendicular to the S -curve (D -axis). Figure 2 de-

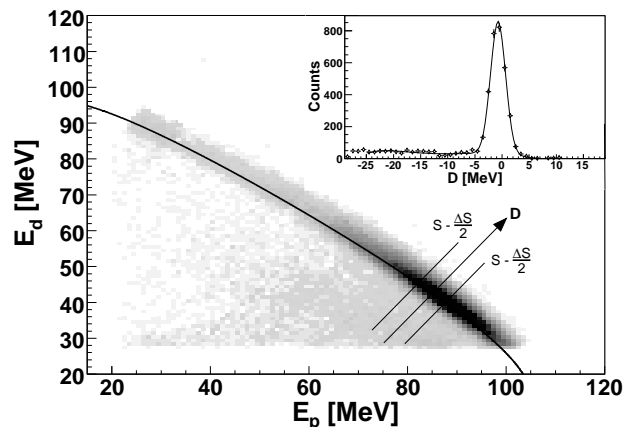


Fig. 2. The correlation between the energies of the deuteron and the proton originating from three-body break-up channel. The projection on the D -axis is shown in the inset.

picts the correlation between the energy of protons and deuterons in coincidence for the kinematical configuration, $(\theta_p, \theta_d, \phi_{12}) = (25^\circ, 25^\circ, 180^\circ)$. The solid curve is the expected correlation for this configuration. One of the many S -intervals and the corresponding D -axis are also shown. The result of the projection of events on the D -axis for a particular S -bin is presented in the inset of Fig. 2. This spectrum consists of mainly break-up events with a negligible amount of accidental background. Particles for most of the break-up events deposit all their energy in the scintillator, which gives rise to a peak around zero for the variable D . Particles in a part of the break-up events undergo a hadronic interaction inside the scintillator or in the material between the target and the detector. For these events the value of S is ill-defined and, therefore, considered as background (primarily to the left-hand side of the main peak in Fig. 2). All the background events were subtracted by fitting a polynomial representing the background and a Gaussian representing the signal to the projected spectrum. The fraction of break-up events which did not deposit their complete energy has been estimated by a GEANT3 simulation and corrected for when determining the cross section.

The interaction of a polarized beam with an unpolarized target produces an azimuthal asymmetry in the scattering cross section. The magnitude of this asymmetry is proportional to the product of the polarization of the beam and an observable that is called the analyzing power. For every kinematical point, ξ , the azimuthal distribution of the scattered particles for a polarized beam is normalized to that of the unpolarized beam. The general expression for the cross section of any reaction induced by a polarized spin-1 projectile is [31,32]:

$$\begin{aligned} \sigma(\xi) = \sigma_0(\xi) & \left[1 + \sqrt{3} p_Z \text{Re}(iT_{11}(\xi)) \cos \phi \right. \\ & - \frac{1}{\sqrt{8}} p_{ZZ} \text{Re}(T_{20}(\xi)) \\ & \left. - \frac{\sqrt{3}}{2} p_{ZZ} \text{Re}(T_{22}(\xi)) \cos 2\phi \right]. \end{aligned} \quad (1)$$

where σ , σ_0 are the polarized and unpolarized cross sections, respectively, ξ represents the configuration $(S, \theta_p, \theta_d, \phi_{12})$. Note that Eq. 1 does not contain terms with $\text{Im}(iT_{11})$, $\text{Re}(T_{21})$, and $\text{Im}(T_{21})$. These contributions vanish because we took explicitly $\beta = 90^\circ$ and $\phi_{12} = |\phi_1 - \phi_2|$. The angle β is the angle between the polarization axis and the momentum of the incoming beam. In this work, the variables $\text{Re}(iT_{11})$, $\text{Re}(T_{20})$ and $\text{Re}(T_{22})$ will be referred to as iT_{11} , T_{20} and T_{22} , respectively. The parameters iT_{11} and p_Z are the vector-analyzing power and the vector beam polarization, respectively. The observables T_{20} and T_{22} are the tensor-analyzing powers, p_{ZZ} is the tensor polarization of the beam, and ϕ is the azimuthal scattering angle of the deuteron.

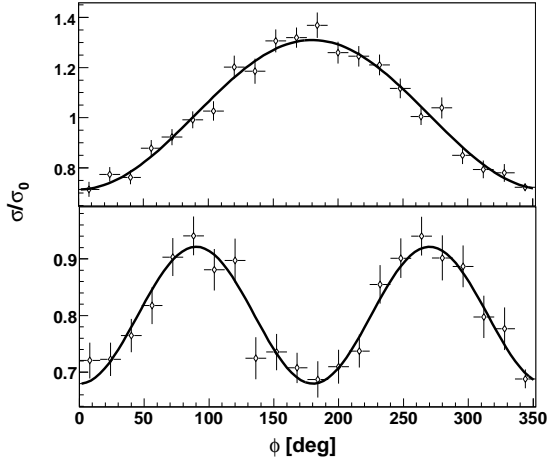


Fig. 3. The ratio of the spin-dependent cross section to the unpolarized one for a pure vector-polarized deuteron beam (top panel) and a pure tensor-polarized deuteron beam (bottom panel) for $(\theta_p = 28^\circ, \theta_d = 30^\circ, \phi_{12} = 180^\circ, S = 210 \text{ MeV})$.

According to Eq. 1, for a deuteron beam with a pure vector polarization, the ratio $\frac{\sigma}{\sigma_0}$ should show a $\cos \phi$ distribution. When a pure tensor-polarized deuteron beam is

used, the ratio $\frac{\sigma}{\sigma_0}$ should show a $\cos 2\phi$ distribution. These asymmetries are exploited to extract the vector-analyzing power, iT_{11} and the tensor-analyzing powers, T_{20} and T_{22} , for every kinematical configuration, $(\theta_p, \theta_d, \phi_{12}, S)$.

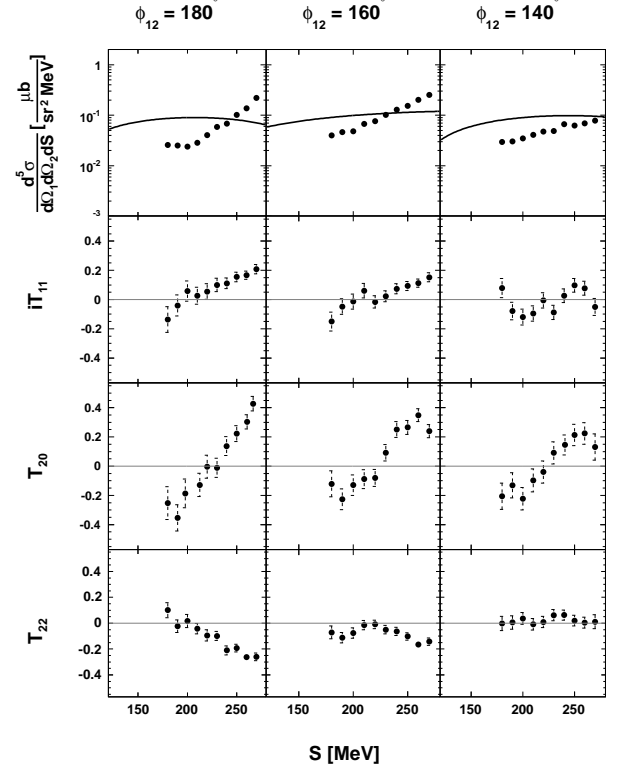


Fig. 4. The cross sections, vector-, and tensor-analyzing powers at $(\theta_d, \theta_p) = (15^\circ, 15^\circ)$ as a function of S for different azimuthal opening angles. The solid curves in the top panels correspond to phase-space distributions. They have arbitrary normalization with respect to the data. The gray lines in other panels show the zero level of the analyzing powers. Only statistical uncertainties are indicated.

Figure 3 shows the ratio $\frac{\sigma}{\sigma_0}$ for a pure vector-polarized deuteron beam (top panel) and a pure tensor-polarized deuteron beam (bottom panel) for $(\theta_p = 28^\circ, \theta_d = 30^\circ, \phi_{12} = 180^\circ, S = 210 \text{ MeV})$. The curves in the top and bottom panels are the results of a fit based on Eq. 1 through the obtained asymmetry distribution for a beam with a pure vector and tensor polarization, respectively. The amplitude of the $\cos \phi$ modulation in the top panel equals $\sqrt{3} p_Z iT_{11}$ and the amplitude of the $\cos 2\phi$ modulation in the lower panel equals $-\frac{\sqrt{3}}{2} p_{ZZ} T_{22}$. The offset from 1 in the lower panel equals $-\frac{1}{\sqrt{8}} p_{ZZ} T_{20}$. The polarization values have been measured independently using BINA and verified by measurements using a Lamb-Shift polarimeter [31], and were found to be $p_Z = -0.601 \pm 0.029$ and $p_{ZZ} = -1.517 \pm 0.032$.

The differential cross section and vector- and tensor-analyzing powers of a few kinematical configurations of the three-body break-up reaction are obtained. The differ-

ential cross sections were compared with a phase-space distribution obtained from a Monte Carlo simulation based on the GEANT3 framework. This comparison demonstrates that there are large variations in the dynamic part of the t -matrix as a function of S for different configurations.

Figure 4 represents the cross sections, vector-, and tensor-analyzing powers at $(\theta_d, \theta_p) = (15^\circ, 15^\circ)$ as a function of S for different azimuthal opening angles. The solid curves in the top panels correspond to phase-space distributions. They have arbitrary normalization with respect to the data. The gray lines in other panels show the zero level of the analyzing powers. Only statistical uncertainties are indicated. The total systematic uncertainty for the cross sections and analyzing power are estimated to be $\sim 7\%$ and $\sim 4.5\%$, respectively.

The three-body break-up reaction in deuteron-deuteron scattering has been identified uniquely using the scattering angles, θ_d, θ_p , the energies and the TOF information of the scattered particles. In this work, we analyzed a part of the data in which both protons and deuterons scattered into the forward wall of BINA. The performed four-body scattering experiments with BINA and the BBS provide an extensive database for the elastic and transfer channels at 65 MeV/nucleon and 90 MeV/nucleon and also for the three-body break-up reaction at 65 MeV/nucleon. The available dataset for the deuteron-deuteron scattering at intermediate energies can be used to check the upcoming theoretical calculations for the four-body systems.

References

1. H. Yukawa, Proc. Phys. Math. Soc. Jap. **17**, (1935) 48
2. L. D. Faddeev, Sov. Phys. JETP. **12**, (1961) 1014
3. W. Glöckle and H. Witała and D. Hüber and H. Kamada and J. Golak, Physics Reports **274**, (1996) 107
4. R. B. Wiringa, A. R. Smith, and T. L. Ainsworth, Phys. Rev. C. **29**, (1984) 1207
5. H. Primakoff, and T. Holstein, Phys. Rev. **55**, (1939) 1218
6. K. Ermisch, *et al.*, Phys. Rev. Lett. **86**, (2001) 5862
7. K. Ermisch, *et al.*, Phys. Rev. C **68**, (2003) 051001
8. K. Ermisch, *et al.*, Phys. Rev. C **71**, (2005) 064004
9. H. Sakai, *et al.*, Phys. Rev. Lett. **84**, (2000) 5288
10. K. Sekiguchi, *et al.*, Phys. Rev. Lett. **95**, (2005) 162301
11. H. Shimizu, *et al.*, Nucl. Phys. A **382**, (1982) 242
12. H. Mardanpour, *et al.*, Eur. Phys. J. A **31**, (2007) 383
13. E. Stephan, *et al.*, Phys. Rev. C **76**, (2005) 057001
14. H. Hatanaka, *et al.*, Eur. Phys. J. A **18**, (2003) 293
15. K. Kuroda, A. Michalowicz, M. Poulet, Nucl. Phys. **88**, (1966) 33
16. R. E. Adelberger, C. N. Brown, Phys. Rev. D **5**, (1972) 2139
17. H. Postma and R. Wilson, Phys. Rev. **121**, (1961) 1129
18. R. Bieber, *et al.*, Phys. Rev. Lett. **84**, (2000) 606
19. K. Sekiguchi, *et al.*, Phys. Rev. C **70**, (2004) 014001
20. H. Mardanpour, PhD. thesis, University of Groningen (2008)
21. H. Amir-Ahmadi, *et al.*, Phys. Rev. C **75**, (2007) 041001
22. M. Eslami-Kalantari, PhD. thesis, University of Groningen (2009)
23. F. Ciesielski and J. Carbonell and C. Gignoux, Phys. Lett. B **447**, (1999) 199
24. A. C. Fonseca, Phys. Rev. Lett **83**, (1999) 4021
25. M. Viviani, A. Kievsky, S. Rosati, E. A. George, and L. D. Knutson, Phys. Rev. Lett **86**, (2001) 3739
26. R. Lazauskas, J. Carbonell, A. C. Fonseca, M. Viviani, A. Kievsky, and S. Rosati, Phys. Rev. C **71**, (2005) 034004
27. C. Alderliesten, A. Djaloeis, J. Bojowald, C. Mayer-Böricke, G. Paic, and T. Sawada, Phys. Rev. C **18**, (1978) 2001
28. V. Bechtold, L. Friedrich, M. S. Abdel-Wahab, J. Bialy, M. Junge, and F. K. Schmidt, Nucl. Phys. A **288**, (1977) 189
29. M. Garcon, *et al.*, Nucl. Phys. A **458**, (1986) 287
30. A. Ramazani-Moghaddam-Arani, *Cross-section and analyzing-power measurements in three and four-nucleon scattering* (PhD thesis, University of Groningen, 2009) 73
31. G. G. Ohlsen, Rep. Prog. Phys. **35**, (1972) 717
32. G. G. Ohlsen, Nucl. Instr. Meth. **179**, (1981) 283

BOSS

bonn